HHS Public Access

Author manuscript

Chem Commun (Camb). Author manuscript; available in PMC 2021 March 12.

Published in final edited form as:

Chem Commun (Camb). 2020 March 12; 56(21): 3163–3166. doi:10.1039/d0cc00108b.

Synthesis and Electronic Structure Studies of a Cr-Imido Redox Series

Yuyang Dong, **Ryan M. Clarke**, **Shao-Liang Zheng**, **Theodore A. Betley**[a]

[a]Department of Chemistry and Chemical Biology, Harvard University, 12 Oxford Street, Cambridge, Massachusetts 02138, United States

Abstract

The effect of metal identity, d-electron count, and coordination geometry on the electronic structure of a metal-ligand multiple bond (MLMB) is an area of active exploration. Although high oxidation state Cr imido have been extensively studied, very few reports on low-valent Cr imidos or the interconversion of redox isomers exist. Herein, we report the synthesis and characterization of a family of dipyrrinato Cr imido complexes in oxidation states ranging from Cr^{III} to Cr^{V}, showcasing the influence of the weak-field dipyrromethene scaffold on the electronic structure and coordination geometries of these Cr imides.

Correlating the electronic structure of metal-ligand multiply bonded complexes to their reactivity is an area of active exploration.[1–16] In 2011, we reported the synthesis of Fe^{III} iminyl complexes competent for C−H amination.[1] These species are best described as high-spin ferric centres antiferromagnetically coupled to an iminyl radical, leading to a $S = 2$ overall ground state.[1, 3–5] The iminyl electronic structure was proposed to result from the compressed ligand field caused by the dipyrrin ligand. Following this report, we have described the syntheses, characterization, and C–H activation reactivity of Co,[2, 6–7] Ni[19] and Cu[8] nitrenoids (i.e., imidos, NR^{2-}; iminyls, $^{2}NR^{-}$; nitrenes ^{3}NR) supported by dipyrrinato ligands. Given the propensity for the Fe, Co, Ni, and Cu complexes to possess unusual open-shell configurations, we were thus interested to examine if early transition metal analogues would possess unusual electronic structures[9] or those more typical of traditional metal-ligand multiple bonds.[20] Given the range of accessible oxidation states that chromium possesses, we targeted dipyrrin Cr complexes and investigated their ability to stabilize Cr imido units. Most reports of Cr imidos feature high-oxidation state species,[10, 21–29] while comparatively fewer reports describe Cr^{IV} complexes[9, 29–33] and a single report of unambiguous Cr^{III}.[34] Herein, we report the synthesis and characterization for a family of Cr imido complexes featuring different oxidation states as well as coordination geometries.

Due to the broad ^{1}H NMR spectroscopic features typical for open-shell Cr complexes, a recently reported dipyrrin (^{AdF}LH) featuring perfluorophenyl substituent at the *meso*

Conflicts of interest

There are no conflicts to declare

†Electronic Supplementary Information (ESI) available. CCDC reference numbers 1967093–1967098. For ESI and crystallographic data in CIF or other electronic format see DOI: 10.1039/x0xx00000x

position was selected (^{AdF}LH: 1,9-di(1-adamantyl)-5-perfluorophenyldipyrrin; See SI, Supplementary Information).[19] Treatment of **1** (^{AdF}LLi) with $CrCl_2(THF)_2$ in THF at −35 °C resulted in an instantaneous colour change from dark yellow to dark orange. Three broad features were observed in the ^{19}F NMR spectrum of the reaction mixture, indicating either free rotation of the perfluorophenyl ring or symmetric coordination environment around the Cr centre. Removal of THF in *vacuo* produced a deep pink solid signifying a coordination change. Indeed, the ^{19}F NMR spectrum of this pink solid dissolved in C_6D_6 displayed five broad signals. Single crystals of the reaction product suitable for X-ray diffraction were grown from a concentrated solution in benzene at room temperature. The product was revealed to be a Cl-bridged, dimeric complex $[(^{AdF}L)CrCl]_2$ (**2**, Figure S9) displaying a square planar environment around each Cr^{II} centre. The Cr–Cr distances are 3.5426(11) Å and 3.5551(10) Å in the two molecules present in the asymmetric unit. The Cr–Cr distances are significantly longer than Cr_2 dimers supported by alkoxides and siloxides with similar structures, indicating the absence of significant Cr–Cr bonding interactions.[30, 35] The same orientation of the dipyrrinato ligands can be attributed to **π-π** stacking in the crystal lattice.

Treatment of **1** with $Cr(OTf)_2$ in THF at −35 °C resulted in a similar colour change to dark orange as further corroborated by UV-Vis spectroscopy (Figure S1). Unlike with complex **2**, no significant colour change was observed upon removal of volatiles. X-ray quality crystals were obtained by storing a concentrated solution of the orange solid residue in a mixture of *n*-hexane/THF at −35 °C overnight. The solid-state molecular structure revealed the product to be the five-coordinate, bis-solvento adduct $(^{AdF}L)Cr(OTf)(thf)_2$ (**3**, Figure S10), which possesses a trigonal-bipyramidal (tbp) environment around the Cr centre with two THF molecules occupying the axial positions. We propose **3** remains solvated unlike complex **2** due to the enhanced electrophilicity imparted by the triflate ion, as well as the diminished propensity for triflate to bridge adjacent metals relative to the chlorides in **2**.

To prepare a low-valent Cr synthon that could give access to low-valent Cr imides,[34] **2** was investigated electrochemically to reveal a pseudo-reversible reductive event at −1.95 V in THF (vs Fc^+/Fc, Figure S2). Given the reduction potentials observed, treatment of either **2** or **3** with one equivalent of KC_8 in thawing THF resulted in an instantaneous colour change from deep orange to deep purple. The colour is not persistent upon warming the solution to −35 °C, whereupon free ligand and additional unidentified species are detected by ^{19}F NMR spectroscopy. Electron paramagnetic resonance (EPR) spectroscopy of an instantly frozen 2-methyltetrahydrofuran solution of the transiently stable, unidentified species **4** revealed an $S = {}^3/_2$ signal (Figure S3). The quartet electronic configuration is consistent with a similar, low-valent Cr^I synthon prepared by Theopold et al.[36] Attempts to isolate **4** were thwarted by its apparent thermal instability. Warming the reduction product to room temperature resulted in the appearance of free ligand by ^{19}F NMR and the presence of multiple paramagnetic species. Due to the apparent thermal instability of **4**, further characterization of its physical and electronic structure is not readily accessible.

Despite the instability of **4**, the transiently stable Cr^I synthon **4** was generated and used *in situ*. When **4** was treated with one equivalent of mesitylazide ($MesN_3$) in benzene, the ^{19}F NMR spectrum of the crude reaction mixture revealed the presence of one major paramagnetic species along with free ligand and multiple paramagnetic species signifying

decomposition. Storing a concentrated *n*-hexane solution of the product mixture at −35 °C overnight afforded X-ray quality crystals to identify the major paramagnetic species as the tetrahedral Cr^{V} bis-imido (^{AdF}L)Cr(NMes)$_2$ (**5**). The solid-state structure of **5** (Figure 1a) reveals Cr−N_{im} bond lengths of 1.677(3) Å and 1.682(3) Å, consistent with previously reported tetragonal Cr^{V} bis-imido complexes supported by *β*-diketiminates.[10, 22] The EPR spectrum of **5** shows an $S = {}^{1}/_{2}$ signal (g = [1.98, 1.97, 1.93], Figure 2). Treatment of the Cr^{I} species *in situ* with two equivalents of $MesN_3$ instantaneously resulted in quantitative conversion to **5**, as confirmed by ^{19}F NMR and EPR spectroscopies as well as X-ray diffraction (Scheme 1). Based on these observations, we propose that a Cr^{III} imido intermediate is likely formed upon mixing **4** with $MesN_3$ which is rapidly trapped by an additional equivalent of azide to generate **5**.

Given the difficulties in preparing a Cr^{III} imide from the Cr^{I} species, we chose to examine whether the target complex could be generated from chemical reduction of the corresponding Cr^{IV} imide. Treatment of **2** with one equivalent of AdN_3 shows no reaction (100 °C, 72 h), where only minor decomposition (determined by the appearance of free ligand by ^{19}F NMR) of **2** is observed with prolonged heating at elevated temperature. Heating **2** with stoichiometric amounts of $MesN_3$ at 100 °C overnight resulted in gradual colour change from dark pink to deep maroon. The ^{19}F NMR spectrum revealed quantitative formation of a new, paramagnetically-shifted species. Storing a concentrated solution of this product in *n*-hexane at −35 °C overnight yielded deep maroon needle-shaped crystals, which were characterized by X-ray diffraction to reveal a terminally bound Cr^{IV} imido species (^{AdF}L)Cr(NMes)Cl (**6**, Scheme 1). The ^{1}H NMR spectroscopy exhibits paramagnetically-shifted broad features, indicating a triplet configuration at room temperature. The solid-state molecular structure of **6** (Figure 1b) displays a tetrahedral environment around the Cr centre. The Cr–N_{im} bond length is 1.640(5) Å along with a slightly bent ∠Cr–N_{im}–C_{Ar} angle of 164.4(4)°, similar to those previously reported for Cr^{IV} imides.[9, 30–33]

With the different coordination geometries observed for **2** and **3** arising from the change in anion, we anticipated a Cr^{IV} imido species with triflate ion bound would adopt a different geometry. Indeed, following a similar procedure used to prepare **6** with triflate starting material **3** yielded a five- coordinate imido (^{AdF}L)Cr(NMes)(OTf)(thf) (**7**) in a tbp geometry (Figure 1c). The average Cr–N_{im} bond length of 1.665(8) Å (two molecules per asymmetric unit) and slightly bent ∠Cr– N_{im}–C_{Ar} average angles of 167.2(9)° are comparable yet elongated relative to those observed in **6** and may be attributable to the larger coordination number around the Cr^{IV} centre. Interestingly, the imido moiety in **7** occupies an axial position in contrast to most tbp MLMB complexes which feature the metal-ligand multiple bond moieties in the equatorial plane.[11, 37] To the best of our knowledge, there are remarkably few tbp complexes featuring the metal-ligand multiply bound moiety in an axial position while possessing more than one d-electron.[38] Orienting the imido unit in the axial position for **7** would result in population of the two d electrons in the d_{xz} and d_{yz} orbitals which are Cr–N_{im} **π***.

With complexes **6** and **7** in hand, we examined their reduction to assess whether a Cr^{III} imide was isolable. Complexes **6** and **7** were subjected to one equivalent of KC_8 in THF at frozen-thawing temperature, resulting in an instantaneous colour change from deep maroon

to dark pink. The ^{19}F NMR spectra revealed the formation of the same species regardless of the starting imide **6** or **7**. Crystals suitable for single-crystal X-ray diffraction grown from a THF/hexanes mixture confirm the loss of anion to generate (^{AdF}L)Cr(NMes)(thf) (**8**, Scheme 1). The Cr^{III} adopts a distorted trigonal pyramidal geometry with the NMes imido moiety in the plane of dipyrrinato ligand, bisecting the adamantyl units. The solid-state structure of **8** (Figure 1d) displays a slightly bent ∠Cr–N_{im}–C_{Ar} angle of 173.0(2)° and Cr–N_{im} bond length of 1.709(3) Å, significantly longer than the sole other trivalent Cr imido species (1.687(2) Å) supported by trispyrrazoleborate (Tp) by Theopold.[34] The zwitterionic nature of the Tp-supported Cr^{III} imide could engender a more electrophilic Cr centre, leading to a shortened Cr-N_{im} bond. Alternatively, the non-tetrahedral geometry of **8** gives rise to non-degenerate Cr-N_{im} **π**-bonding orbitals, which may lead to a diminished Cr-N_{im} bond order as compared to the Tp-analogue. The Cr–N_L distances are 2.101(3) Å and 2.100(3) Å, significantly longer than those in **6** and **7**, consistent with a more reduced Cr^{III} centre. The EPR spectroscopy of **8** shows an $S = {}^3/_2$ signal (g_{iso} = 1.98, |E/D| = 0.01, Figure 3), with a minor $S = {}^1/_2$ signal matching that of **5**. Leaving an *n*-hexane solution of **8** at −35 °C for a week results in complete conversion of **8** to **5** along with concomitant decomposition (i.e., appearance of free ligand) as observed by ^{19}F NMR spectroscopy, whereas a THF solution of **8** is stable for weeks at −35 °C. Thus, the instability of **8** is potentially attributable to slow dissociation of the bound THF followed by disproportionation to **5** and an ill-defined Cr^{I} byproduct. Treatment of **8** with one additional equivalent of $MesN_3$ in C_6D_6 resulted in instantaneous conversion to **5** as confirmed by EPR and ^{19}F NMR spectroscopies as well as X-ray diffraction. Similar reactivity was observed with previously reported Fe and Co analogues, albeit tetrazyl products were formed as opposed to the generation of a bis-imido.[2, 4, 6]

To corroborate the proposed electronic structures of imidos, geometry optimizations of **6**-**8** were conducted to produce atomic coordinates with which to carry out electronic structure calculations. The complete structures of **6**-**8** were optimized using the UKS B3LYP functional and the def2-svp (C, H, F) and def2-tzvp (Cr, N) basis sets of Ahlrich's.[39–42] The optimized structures accurately reproduced the experimental bond metrics for each complex (Table S1). Electronic structure calculations support the assignment of a high-spin d^2 Cr^{IV} (S = 1) for tetrahedral **6** and tbp **7** with minimal amount of spin contamination. Worth noting, the Cr–N_{im} **π*** interactions from the imido group are more destabilizing than the **σ*** interactions from the weak-field dipyrrin (Figure S6–7). Indeed, the Cr–N_{im} **π*** interactions in **7** raise the energy of the **π**-symmetric d_{xz}, d_{yz} pair to avoid population and reduction of the Cr–N_{im} bond order, leaving the two d electrons to populate the near degenerate, non-bonding orbitals. The optimized structure and frontier molecular orbitals for **8** are presented in Figure S8. As with **6** and **7**, the Cr–N_{im} **π*** interactions are the most destabilizing, exceeding even the imido **σ*** interaction. As a result, the d^3 configuration requires population of the third d-electron in the Cr–N_{im} **σ*** orbital, which may contribute to the reactive nature of **8**. The electronic structure calculations support the assignment of a high-spin d^3 Cr^{III} ($S = {}^3/_2$) with negligible amount of spin contamination. It is worth noting that though the DFT optimized bond metrics accurately match experimental values (Table S1), the NMes moiety is bent out of the plane of the dipyrrin ligand by 38.4° in contrast to the solid-state structure.

In conclusion, we have successfully synthesized a family of dipyrrin Cr imido complexes in oxidation states ranging from Cr^{III} to Cr^{V}, featuring a rare example of a trivalent Cr imido in an unusual distorted trigonal pyramidal geometry. We found that trivalent Cr imido is highly reactive towards organic azides, rapidly converting to a Cr^{V} bis-imido. Electronic structure investigations revealed traditional Cr imide formulations in the d^1-d^3 cases, where the ligand field strength exerted by the imido exceeds all other ligand contributions. The preparation and electrochemical investigation of a series of Cr^{V} species with mixed functionalities as well as the group transfer reactivity of all these Cr imido species are currently under study.

Supplementary Material

Refer to Web version on PubMed Central for supplementary material.

Acknowledgments

This work was supported by a grant from the NIH (GM-115815), the Dreyfus Foundation (Teacher-Scholar Award to T.A.B.), and Harvard University.

Notes and references

1. King ER; Hennessy ET; Betley TA, J. Am. Chem. Soc 2011, 133, 4917–4923. [PubMed: 21405138]
2. King ER; Sazama GT; Betley TA, J. Am. Chem. Soc 2012, 134, 17858–17861. [PubMed: 23043624]
3. Iovan DA; Betley TA, J. Am. Chem. Soc 2016, 138, 1983–1993. [PubMed: 26788747]
4. Wilding MJT; Iovan DA; Betley TA, J. Am. Chem. Soc 2017, 139, 12043–12049. [PubMed: 28777558]
5. Wilding MJT; Iovan DA; Wrobel AT; Lukens JT; MacMillan SN; Lancaster KM; Betley TA, J. Am. Chem. Soc 2017, 139, 14757–14766. [PubMed: 28937756]
6. Baek Y; Betley TA, J. Am. Chem. Soc 2019, 141, 7797–7806. [PubMed: 31016975]
7. Baek Y; Hennessy ET; Betley TA, J. Am. Chem. Soc 2019, 141, 16944–16953. [PubMed: 31550162]
8. Carsch KM; DiMucci IM; Iovan DA; Li A; Zheng S-L; Titus CJ; Lee SJ; Irwin KD; Nordlund D; Lancaster KM; Betley TA, Science 2019, 365, 1138. [PubMed: 31515388]
9. Lu CC; DeBeer George S; Weyhermüller T; Bill E; Bothe E; Wieghardt K, Angew. Chem. Int. Ed 2008, 47, 6384–6387.
10. Tsai Y-C; Wang P-Y; Chen S-A; Chen J-M, J. Am. Chem. Soc 2007, 129, 8066–8067. [PubMed: 17567013]
11. Betley TA; Wu Q; Van Voorhis T; Nocera DG, Inorg. Chem 2008, 47, 1849–1861. [PubMed: 18330975]
12. Wiese S; McAfee JL; Pahls DR; McMullin CL; Cundari TR; Warren TH, J. Am. Chem. Soc 2012, 134, 10114–10121. [PubMed: 22616768]
13. Zhang L; Liu Y; Deng L, J. Am. Chem. Soc 2014, 136, 15525–15528. [PubMed: 25330361]
14. Goswami M; Lyaskovskyy V; Domingos SR; Buma WJ; Woutersen S; Troeppner O; Ivanović-Burmazović I; Lu H; Cui X; Zhang XP; Reijerse EJ; DeBeer S; van Schooneveld MM; Pfaff FF; Ray K; de Bruin B, J. Am. Chem. Soc 2015, 137, 5468–5479. [PubMed: 25844713]
15. Laskowski CA; Miller AJM; Hillhouse GL; Cundari TR, J. Am. Chem. Soc 2011, 133, 771–773. [PubMed: 21175213]
16. Saouma CT; Peters JC, Coord. Chem. Rev 2011, 255, 920–937. [PubMed: 21625302]
17. Hagen WR, Mol. Phys 2007, 105, 2031–2039.
18. Stoll S; Schweiger A, J. Magn. Reson 2006, 178, 42–55. [PubMed: 16188474]
19. Dong Y; Lukens JT; Clarke RM; Zheng S-L; Lancaster KM; Betley TA, Chem. Sci 2020.

20. Nugent WA; Mayer JM, Metal-ligand multiple bonds: the chemsitry of transition metal complexes containing oxo, nitrido, imido, or alkylidyne ligands Wiley-Intersicence: New York, 1988.
21. Leung W-H; Wu M-C; Wong TKT; Wong W-T, Inorg. Chim. Acta 2000, 304, 134–136.
22. Monillas WH; Yap GPA; Theopold KH, Inorg. Chim. Acta 2011, 369, 103–119.
23. Danopoulos AA; Hankin DM; Wilkinson G; Cafferkey SM; Sweet TKN; Hursthouse MB, Polyhedron 1997, 16, 3879–3892.
24. Leung W-H; Wu M-C; L. C. Chim J; Yu M-T; Hou H.-w.; Yeung L-L; Wong W-T; Wang Y, J. Chem. Soc. Dalton Trans 1997, 3525–3529.
25. Chin Chew K; Clegg W; P. Coles M; R. J. Elsegood M; C. Gibson V; J. P. White A; J. Williams D, J. Chem. Soc. Dalton Trans 1999, 2633–2640.
26. Leung W-H; Danopoulos AA; Wilkinson G; Hussain-Bates B; Hursthouse MB, J. Chem. Soc. Dalton Trans 1991, 2051–2061.
27. Lam H.-w.; Wilkinson G; Hussain-Bates B; Hursthouse MB, J. Chem. Soc. Dalton Trans 1993, 1477–1482.
28. Zdilla MJ; Abu-Omar MM, J. Am. Chem. Soc 2006, 128, 16971–16979. [PubMed: 17177448]
29. Zhou W; Patrick BO; Smith KM, Chem. Comm 2014, 50, 9958–9960. [PubMed: 25033731]
30. Sydora OL; Kuiper DS; Wolczanski PT; Lobkovsky EB; Dinescu A; Cundari TR, Inorg. Chem 2006, 45, 2008–2021. [PubMed: 16499361]
31. Barron AR; Salt JE; Wilkinson G; Motevalli M; Hursthouse MB, J. Chem. Soc. Dalton Trans 1987, 2947–2954.
32. Danopoulos AA; Wilkinson G; Sweet TKN; Hursthouse MB, J. Chem. Soc. Dalton Trans 1995, 2111–2123.
33. Danopoulos AA; Wilkinson G; Sweet TKN; Hursthouse MB, Polyhedron 1996, 15, 873–879.
34. Akturk ES; Yap GPA; Theopold KH, Chem. Comm 2015, 51, 15402–15405. [PubMed: 26344782]
35. Yousif M; Tjapkes DJ; Lord RL; Groysman S, Organometallics 2015, 34, 5119–5128.
36. Monillas WH; Young JF; Yap GPA; Theopold KH, Dalton Trans. 2013, 42, 9198–9210. [PubMed: 23493916]
37. Ogba OM; Warner NC; O'Leary DJ; Grubbs RH, Chem. Soc. Rev 2018, 47, 4510–4544. [PubMed: 29714397]
38. England J; Farquhar ER; Guo Y; Cranswick MA; Ray K; Münck E; Que L, Inorg. Chem 2011, 50, 2885–2896. [PubMed: 21381646]
39. Becke AD, J. Chem. Phys 1993, 98, 5648–5652.
40. Becke AD, J. Chem. Phys 1993, 98, 1372–1377.
41. Schäfer A; Horn H; Ahlrichs R, J. Chem. Phys 1992, 97, 2571–2577.
42. Schäfer A; Huber C; Ahlrichs R, J. Chem. Phys 1994, 100, 5829–5835.

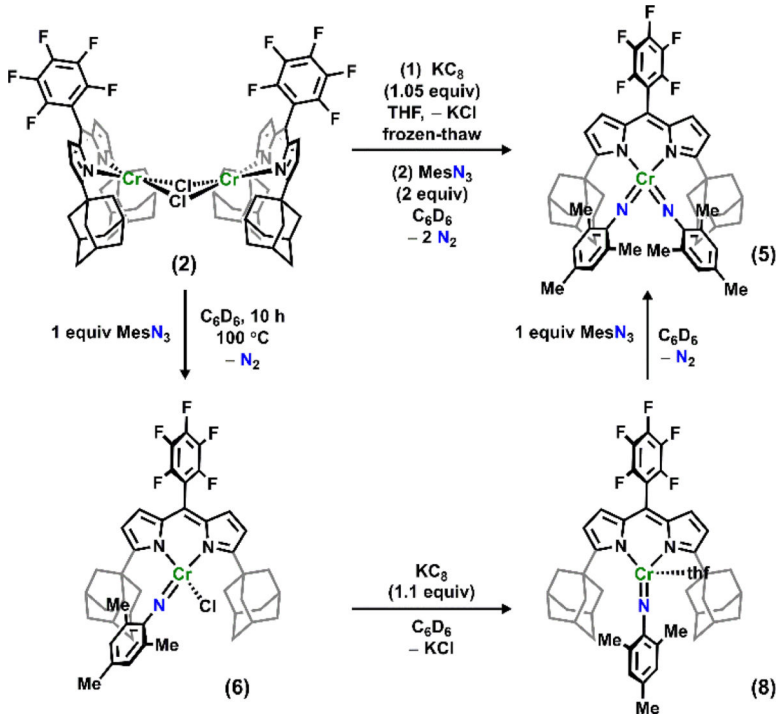

Scheme 1.

Synthesis of imido complexes in this study (^{AdF}L)Cr(NMes)$_2$ (**5**), (^{AdF}L)CrCl(NMes) (**6**) and (^{AdF}L)Cr(NMes)(thf) (**8**) derived from [(^{AdF}L)CrCl]$_2$ (**2**).

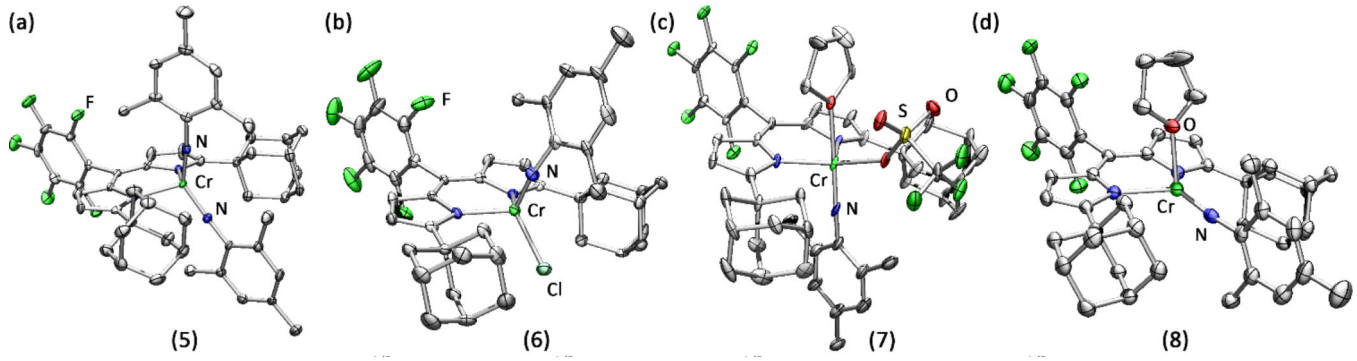

Figure 1.

Solid-state molecular structures for (a) (^{AdF}L)Cr(NMes)$_2$ (**5**), (b) (^{AdF}L)Cr(NMes)Cl (**6**), (c) (^{AdF}L)Cr(NMes)(OTf)(thf) (**7**), and (d) (^{AdF}L)Cr(NMes)(thf) (**8**) with thermal ellipsoids at 50% (a, b, d) and 30% (c) probability level. Colour scheme: Cr, spring green; N, blue; Cl, yellow green; F, green.

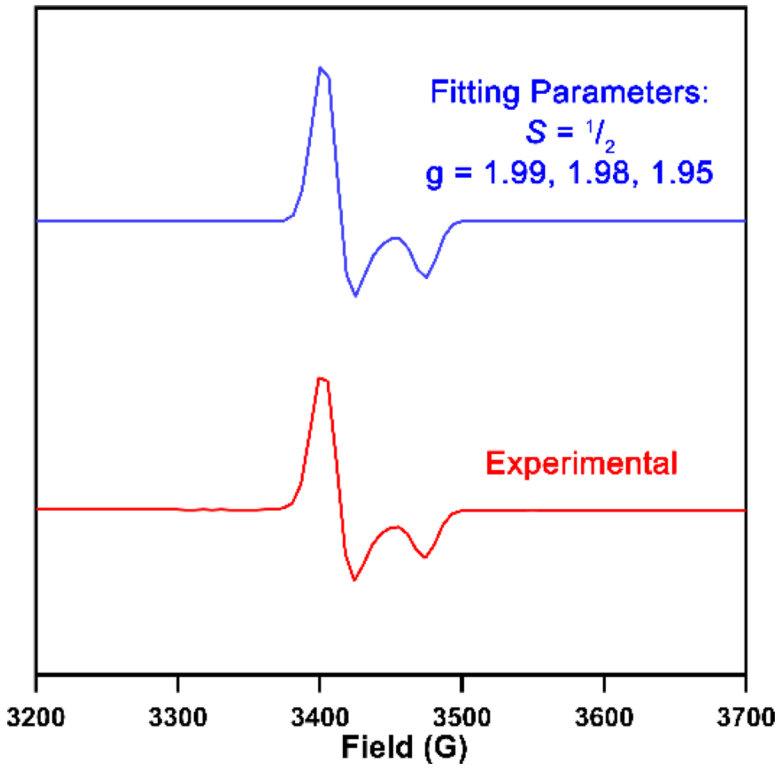

Figure 2.
EPR spectrum of (^{AdF}L)Cr(NMes)$_2$ (**5**) at 77 K. Blue trace: fitted spectrum with EasySpin.[18]

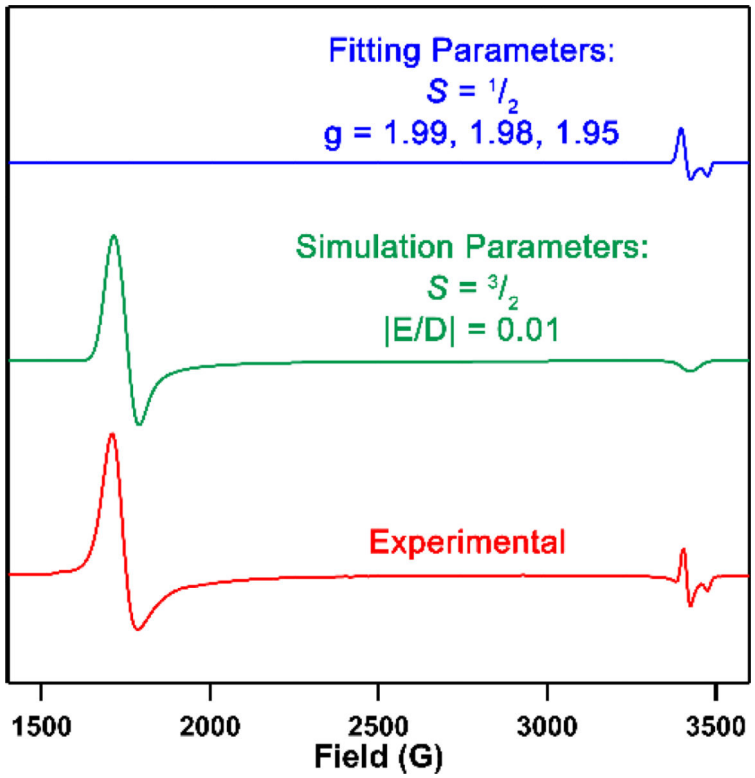

Figure 3.

EPR spectrum of (^{AdF}L)Cr(NMes)$_2$ **5** at 77 K. Green trace: simulated spectrum with VisualRhombo.[17] Blue trace: fitted Cr^V impurity spectrum with EasySpin.[18]